

# Analysis of Breakdown Characteristics in Field-Plate AlGaN/GaN HEMTs: Dependence on Deep-Acceptor Density in Buffer Layer

S. Akiyama, M. Kondo, L. Wada, and K. Horio

Faculty of Systems Engineering, Shibaura Institute of Technology  
307 Fukasaku, Minuma-ku, Saitama 337-8570, Japan, horio@sic.shibaura-it.ac.jp

## ABSTRACT

We make a two-dimensional analysis of field-plate AlGaN/GaN HEMTs with a Fe-doped semi-insulating buffer layer, and studied how the deep-acceptor density in the buffer layer  $N_{DA}$  and the field-plate length  $L_{FP}$  affect the breakdown voltage  $V_{br}$  of AlGaN/GaN HEMTs.  $N_{DA}$  is varied between  $10^{17} \text{ cm}^{-3}$  and  $3 \times 10^{17} \text{ cm}^{-3}$ , and the deep-acceptor's energy level is set 0.5 eV below the bottom of conduction band.  $L_{FP}$  is varied between 0 and 1  $\mu\text{m}$ . The calculated off-state breakdown characteristics show that the drain current usually increases steeply due to impact ionization of carriers, resulting in breakdown. But, in some cases,  $V_{br}$  is determined by buffer leakage current. This current is larger for lower  $N_{DA}$ , and hence  $V_{br}$  becomes higher for higher  $N_{DA}$ . It is also shown that  $V_{br}$  takes a maximum value at  $L_{FP} = 0.2\text{-}0.3 \mu\text{m}$  when the gate-to-drain distance is 1.5  $\mu\text{m}$ , and that the average electric field for breakdown between gate and drain becomes 3.2 MV/cm when  $N_{DA}$  is  $3 \times 10^{17} \text{ cm}^{-3}$ .

**Keywords:** GaN HEMT, field plate, breakdown voltage, buffer layer, deep acceptor

## 1 INTRODUCTION

AlGaN/GaN HEMTs are now receiving great interest for application to high-power microwave devices and high power switching devices [1, 2]. To improve the power performance and the breakdown voltage of FETs, the introduction of field plate is shown to be effective [3-8]. This is because the field plate reduce the current collapse of the FETs, and the electric field at the drain edge of the gate is reduced.

As another method to improve the breakdown voltage of AlGaN/GaN HEMTs, we proposed a structure including a high- $k$  passivation layer, and showed that the breakdown voltage increased significantly. We first assumed an undoped semi-insulating buffer layer where a deep donor compensates a deep acceptor [9, 10]. Recently, Fe- and C-doped semi-insulating buffer layers are often adopted and they acts as deep acceptors [11-15]. Hence, we analyzed AlGaN/GaN HEMTs with a buffer layer including only a deep acceptor, and found that the breakdown voltage became higher when the acceptor density became higher [16].

Therefore, in this work, we make a two-dimensional

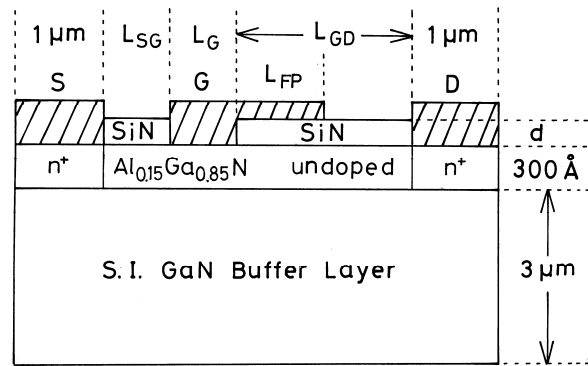


Figure 1: Device structure analyzed in this study.

analysis of breakdown characteristics in field-plate AlGaN/GaN HEMTs with a Fe-doped semi-insulating buffer layer, and study how the breakdown voltage is influenced by the deep acceptor density in the buffer layer.

## 2 PHYSICAL MODEL

A device structure analyzed here is shown in Fig.1. The gate length and the gate-to-drain distance is 0.3  $\mu\text{m}$  and 1.5  $\mu\text{m}$ , respectively. The SiN passivation layer's thickness is 0.1  $\mu\text{m}$ . The field-plate length  $L_{FP}$  is varied between 0 and 1  $\mu\text{m}$ . Here, we adopt a Fe-doped semi-insulating buffer layer, where the Fe-related level ( $E_{DA}$ ) is set to 0.5 eV below the bottom of conduction band [11, 15]. The Fe-related level is a deep acceptor. The deep acceptors act as electron traps. The deep-acceptor density  $N_{DA}$  is varied between  $10^{17}$  and  $3 \times 10^{17} \text{ cm}^{-3}$ .

Basic equations to be solved are Poisson's equation having the ionized deep-acceptor density term and electron and hole continuity equations which include a carrier loss rate via the deep acceptor and an impact ionization rate [10, 16-19] and expressed as follows.

1) Poisson's equation

$$\nabla \bullet (\epsilon \nabla \psi) = -q(p - n + N_{Di} - N_{DA}^-) \quad (1)$$

2) Continuity equations for electrons and holes

$$\nabla \bullet J_n = -qG + qR_{DA} \quad (2)$$

$$\nabla \bullet J_p = qG - qR_{DA} \quad (3)$$

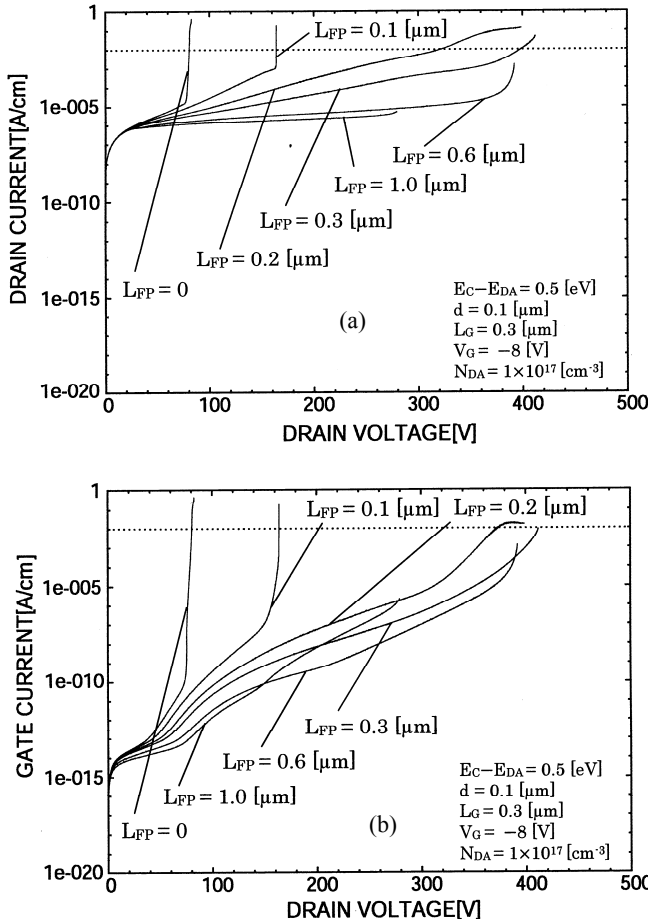


Figure 2: Calculated  $I_D$ - $V_D$  curves and (b)  $I_G$ - $V_D$  curves of AlGaN/GaN HEMT with  $N_{DA} = 10^{17} \text{ cm}^{-3}$ .

where  $N_{DA}^-$  is the ionized deep-acceptor density, and  $R_{DA}$  represents a carrier recombination rate via the deep acceptor.  $G$  is a carrier generation rate by impact ionization, and given by

$$G = (\alpha_n |J_n| + \alpha_p |J_p|)/q \quad (4)$$

where  $\alpha_n$  and  $\alpha_p$  are ionization rates for electrons and holes, respectively, and expressed as

$$\alpha_n = A_n \exp(-B_n / |E|) \quad (5)$$

$$\alpha_p = A_p \exp(-B_p / |E|) \quad (6)$$

where  $E$  is the electric field.  $A_n$ ,  $B_n$ ,  $A_p$ , and  $B_p$  are deduced from [20].

The above basic equations are put into discrete forms and solved numerically.

### 3 RESULTS AND DISCUSSIONS

Figs.2 and 3 show calculated (a) drain current  $I_D$  – drain voltage  $V_D$  curves and (b) gate current  $I_G$  –  $V_D$  curves of field-plate AlGaN/GaN HEMTs with the field-plate length  $L_{FP}$  as a parameter. Fig.2 show the case of  $N_{DA} = 10^{17} \text{ cm}^{-3}$

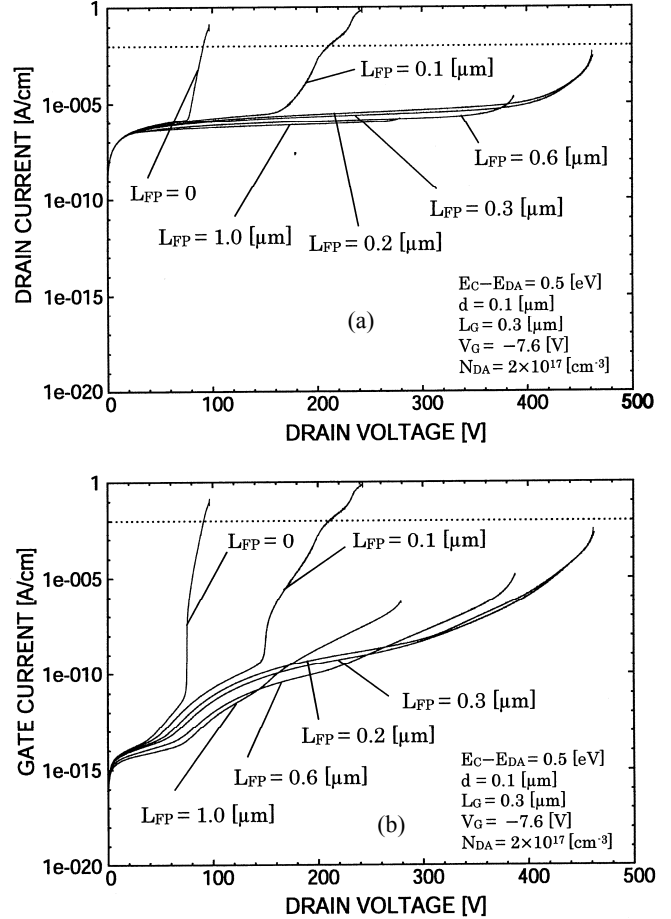


Figure 3: Calculated  $I_D$ - $V_D$  curves and (b)  $I_G$ - $V_D$  curves of AlGaN/GaN HEMT with  $N_{DA} = 2 \times 10^{17} \text{ cm}^{-3}$ .

and Fig.3 shows the case of  $N_{DA} = 2 \times 10^{17} \text{ cm}^{-3}$ . In Fig.2, the gate voltage  $V_G$  is  $-8 \text{ V}$  and in Fig.3,  $V_G$  is  $-7.62 \text{ V}$ . These voltages are  $V_{th} - 2 \text{ V}$  where  $V_{th}$  is the threshold voltage, so Figs.2 and 3 are off-state breakdown characteristics. At  $L_{FP} = 0$  and  $0.1 \mu\text{m}$ ,  $I_D$  increases suddenly, resulting in breakdown. This is due to an abrupt increase in  $I_G$ , and  $I_D = I_G$  in this region. But, in Fig.2 ( $N_{DA} = 10^{17} \text{ cm}^{-3}$ ), when  $L_{FP} = 0.2 \mu\text{m}$  and  $0.3 \mu\text{m}$ ,  $I_D$  increases gradually and reaches a critical current level ( $10^{-2} \text{ A/cm}$  or  $1 \text{ mA/mm}$ ), and in this case  $I_G$  is rather lower than  $I_D$ . Therefore, in this case the buffer leakage current determines the breakdown voltage. In other cases, the overall increase in  $I_D$  correlates well with the increase in  $I_G$ , and the breakdown voltage is determined by impact ionization of carriers. Here, we define the breakdown voltage as a drain voltage when  $I_D$  becomes  $1 \text{ mA/mm}$  ( $10^{-2} \text{ A/cm}$ ). So, in the cases of  $L_{FP} = 0.2$  and  $0.3 \mu\text{m}$ , the breakdown voltages are higher when  $N_{DA} = 2 \times 10^{17} \text{ cm}^{-3}$ . When  $L_{FP} = 0.6 \mu\text{m}$  and  $1 \mu\text{m}$ ,  $I_D$  does not reach  $1 \text{ mA/mm}$ , but the onset voltages of current rise seems to be similar.

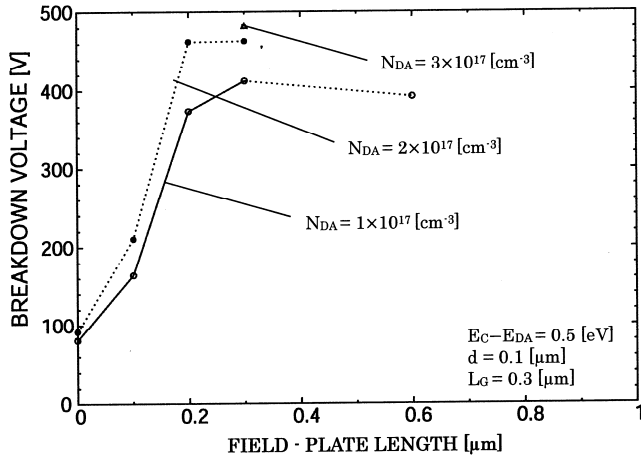


Figure 4: Breakdown voltage as a function of field-plate length  $L_{FP}$ , with  $N_{DA}$  as a parameter.

Fig.4 shows the breakdown voltage  $V_{br}$  versus  $L_{FP}$  curves as a parameter of  $N_{DA}$ . The breakdown voltage is defined here as a drain voltage when  $I_D$  becomes 1 mA/mm. It is clearly seen that  $V_{br}$  becomes higher when  $N_{DA}$  is higher, although several points are missing because  $I_D$  does not reach 1 mA/mm particularly for high  $N_{DA}$ . The higher  $V_{br}$  for higher  $N_{DA}$  should be due to the lower buffer leakage current due to a steeper barrier at the channel-buffer interface [21]. The obtained highest  $V_{br}$  here is about 480 V at  $N_{DA} = 3 \times 10^{17} \text{ cm}^{-3}$  and  $L_{FP} = 0.3 \mu\text{m}$ , which correspond to an average electric field of about 3.2 MV/cm between the gate and the drain. From Fig.4, we also see that there is an optimum  $L_{FP}$  to obtain a high  $V_{br}$ . Fig.5 shows a comparison of electric field profiles between the two cases with (a)  $L_{FP} = 0.3 \mu\text{m}$  and (b)  $L_{FP} = 1 \mu\text{m}$ . Here  $N_{DA} = 2 \times 10^{17} \text{ cm}^{-3}$ . In both cases, the electric field at the drain edge of the gate is reduced, and the voltage is applied between the field-plate edge and the drain. In the case of  $L_{FP} = 1 \mu\text{m}$ , the distance between the field-plate edge and the drain is 0.5  $\mu\text{m}$ , and hence the electric field becomes very high in this region. Therefore, the breakdown voltage at  $L_{FP} = 1 \mu\text{m}$  becomes lower than that for  $L_{FP} = 0.3 \mu\text{m}$ , and the optimum value of  $L_{FP}$  appears.

#### 4 CONCLUSION

A two-dimensional analysis of field-plate AlGaN/GaN HEMTs with a Fe-doped semi-insulating buffer layer has been performed, and it has been studied how the deep-acceptor density in the buffer layer  $N_{DA}$  and the field-plate length  $L_{FP}$  affect the breakdown voltage  $V_{br}$  of AlGaN/GaN HEMTs. The calculated off-state breakdown characteristics have shown that the drain current usually increases steeply due to impact ionization of carriers, resulting in breakdown. But, in some cases,  $V_{br}$  is determined by the buffer leakage current. This current is smaller for higher  $N_{DA}$  due to a

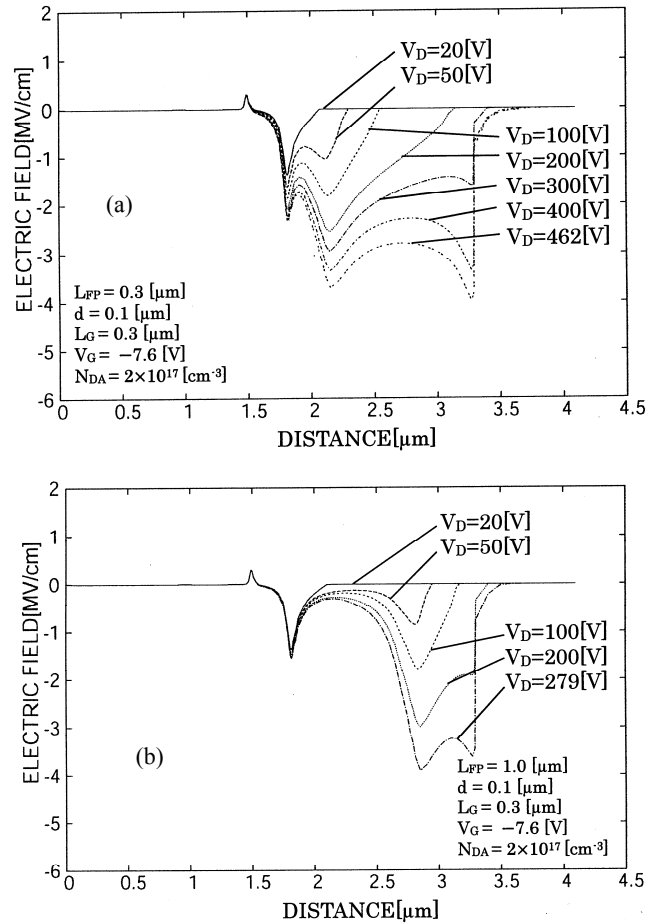


Figure 5: Comparison of electric field profiles between the two cases with (a)  $L_{FP} = 0.3 \mu\text{m}$  and (b)  $L_{FP} = 1 \mu\text{m}$ .  $N_{DA} = 2 \times 10^{17} \text{ cm}^{-3}$ .

steeper barrier at the channel-buffer interface, and hence  $V_{br}$  becomes higher for higher  $N_{DA}$ . It is also shown that  $V_{br}$  takes a maximum value at  $L_{FP} = 0.2\text{-}0.3 \mu\text{m}$  when the gate-to-drain distance is 1.5  $\mu\text{m}$ , and that the average electric field for breakdown between the gate and the drain becomes 3.2 MV/cm when  $N_{DA}$  is  $3 \times 10^{17} \text{ cm}^{-3}$ .

#### REFERENCES

- [1] U. K. Mishra, L. Shen, T. E. Kazior, and Y.-F. Wu, "GaN-based RF power devices and amplifiers", Proc. IEEE, vol.96, pp.287-305, 2008.
- [2] N. Ikeda, Y. Niizuma, H. Kambayashi, Y. Sato, T. Nomura, S. Kato, and S. Yoshida, "GaN power transistors on Si substrates for switching applications", Proc. IEEE, vol.98, pp.1151-1161, 2010.
- [3] A. Wakejima, K. Ota, K. Matsunaga, and M. Kuzuhara, "A GaAs-based field-modulating plate HFET with improved WCDMA peak-output-power characteristics", IEEE Trans. Electron Devices, vol.50, pp.1983-1987, Sep. 2003.

- [4] Y.-F. Wu, A. Saxler, M. Moore, R. P. Smith, S. Sheppard, P. M. Chavarkar, T. Wisleder, U. K. Mishra, and P. Parikh, “30-W/mm GaN HEMTs by field plate optimization”, *IEEE Electron Device Lett.*, vol.25, pp.117-119, 2004.
- [5] K. Horio, A. Nakajima, and K. Itagaki, “Analysis of field-plate effects on buffer-related lag phenomena and current collapse in GaN MESFETs and AlGaN/GaN HEMTs”, *Semicond. Sci. Technol.*, vol.24, pp.085022-1–085022-7, 2009.
- [6] K. Horio, T. Tanaka, K. Itagaki and A. Nakajima, “Two-dimensional analysis of field-plate effects on surface state-related current transients and power slump in GaAs FETs”, *IEEE Trans. Electron Devices*, vol.58, pp. 698-703, 2011.
- [7] S. Karmalkar and U. K. Mishra, “Enhancement of breakdown voltage in AlGaN/GaN high electron mobility transistors using a field plate”, *IEEE Trans. Electron Devices*, vol.48, pp.1515-1521, 2001.
- [8] H. Onodera and K. Horio, “Analysis of buffer-impurity and field-plate effects on breakdown characteristics in small sized AlGaN/GaN high electron mobility transistors”, *Semicond. Sci. Technol.*, vol.27, pp.085016-1–085016-6, 2012.
- [9] H. Hanawa and K. Horio, “Increase in breakdown voltage of AlGaN/GaN HEMTs with a high- $k$  dielectric layer”, *Phys. Status Solidi A*, vol.211, pp.784-787, 2014.
- [10] H. Hanawa, H. Onodera, A. Nakajima, and K. Horio, “Numerical analysis of breakdown voltage enhancement in AlGaN/GaN HEMTs with a high- $k$  passivation layer”, *IEEE Trans. Electron Devices*, vol.61, pp.769-775, 2014.
- [11] M. Silvestri, M. J. Uren, and M. Kuball, “Iron-induced deep-acceptor center in GaN/AlGaN high electron mobility transistors: Energy level and cross section”, *Appl. Phys. Lett.* Vol.102, pp.073051-1–073051-4, 2013.
- [12] G. Verzellesi, L. Morassi, G. Meneghesso, M. Meneghini, E. Zanoni, G. Pozzovivo, S. Lavanga, T. Detzel, O. Häberlen, and G. Curatola, “Influence of carbon doping on pulsed and AC behavior of insulated-gate field-plated power AlGaN/GaN HEMTs”, *IEEE Electron Device Lett.* vol.35, pp.443-445, 2014.
- [13] S. Gusafsson, Jr-T. Chen, J. Bergten, U. Forsberg, M. Thorsell, E. Janzén, and N. Rorsman, “Dispersive effects in microwave AlGaN/AlN/GaN HEMTs with carbon-doped buffer”, *IEEE Trans. Electron Devices*, vol.62, pp.2162-2169, 2015.
- [14] J. Hu, S. Stoffels, S. Lenci, G. Groeseneken, and S. Decoutere, “On the identification of buffer trapping for bias-dependent dynamic  $R_{ON}$  of AlGaN/GaN Schottky barrier diode with AlGaN:C back barrier”, *IEEE Electron Device Lett.*, vol.37, pp.310-313, 2016.
- [15] Y. S. Puzyrev, R. D. Schrimpf, D. M. Fleetwood, and S. T. Pantelides, “Role of Fe impurity complexes in the degradation of GaN/AlGaN high-electron mobility transistors”, *Appl. Phys. Lett.*, vol.106, pp.053505-1–053505-4, 2015.
- [16] T. Kabemura, S. Ueda, Y. Kawada, and K. Horio, “Enhancement of breakdown voltage in AlGaN/GaN HEMTs: Field plate plus high- $k$  passivation layer and high acceptor density in buffer layer”, *IEEE Trans. Electron Devices*, vol.65, no.9, pp.3848-3854, 2018.
- [17] K. Horio and K. Satoh, “Two-dimensional analysis of substrate-related kink phenomena in GaAs MESFET’s”, *IEEE Trans. Electron Devices*, vol.41, pp.2256-2261, 1994.
- [18] K. Horio and A. Wakabayashi, “Numerical analysis of surface-state effects on kink phenomena of GaAs MESFETs”, *IEEE Trans. Electron Devices*, vol.47, pp.2270-2276, 2000.
- [19] Y. Mitani, D. Kasai and K. Horio, “Analysis of surface-state and impact-ionization effects on breakdown characteristics and gate-lag phenomena in narrowly-recessed-gate GaAs FETs”, *IEEE Trans. Electron Devices*, vol.50, pp.285-291, 2003.
- [20] C. Bulutay, “Electron initiated impact ionization in AlGaN alloys”, *Semicond. Sci. Technol.*, vol.17, pp.59-62, 2002.
- [21] Y. Saito, R. Tsurumaki, N. Noda and K. Horio, “Analysis of reduction in lag phenomena and current collapse in field-plate AlGaN/GaN HEMTs with high acceptor density in a buffer layer”, *IEEE Trans. Device Mater. Rel.*, vol.18, no.1, pp.46-53, 2018.